

# Plasma Equilibrium in Tokamaks

J.P. Goedbloed

FOM-Institute for Plasma Physics ‘Rijnhuizen’, Association Euratom-FOM  
P.O.Box 1207, 3430 BE Nieuwegein, The Netherlands

&  
Astronomical Institute, Utrecht University

## 1 Introduction

The task of the theory of tokamak equilibrium is *to determine the global magnetic confinement topology* and physical characteristics of the underlying basic equilibrium state, which is assumed to be static (both  $\partial/\partial t = 0$  and background velocity  $\mathbf{v}_0 = 0$ ). This could be considered to be the most boring case of plasma behavior, viz. total absence of dynamics: a corresponding fluid dynamics problem hardly exists. The reason for our interest in this plasma state is the prospect of obtaining clean, abundant, and cheap energy from controlled thermonuclear fusion reactions. Of course, criticism and doubt immediately enter the mind after a statement like this. Nevertheless, let us study this plasma state, leaving questions like ‘is there such a state at all?’ and ‘is it actually so desirable?’ for later (Sec. 5).

The MHD equilibrium equations are about the best satisfied plasma equations we know. If a plasma is sitting at rest it is hard to imagine it satisfying any other conditions than the following ones:

$$\mathbf{j} \times \mathbf{B} = \nabla p \quad (\textit{pressure balance}), \quad (1)$$

$$\mathbf{j} = \frac{1}{\mu_0} \nabla \times \mathbf{B} \quad (\textit{Ampère's law}), \quad (2)$$

$$\nabla \cdot \mathbf{B} = 0 \quad (\textit{THE law of magnetic fields}). \quad (3)$$

Indeed, if these equations are not satisfied the plasma is instantaneously accelerated to huge velocities and there is no way to prevent it being smashed into the wall of the confinement vessel.

Historically, the subject of plasma equilibrium is associated with the unsuccessful early attempts (by the very same people who had been so ‘successful’ unleashing the fusion energy on our planet) with the simple schemes of  $\theta$ - and  $z$ -pinch, easily producing the temperatures needed for thermonuclear ignition but falling short by a factor of a million to a billion with respect to confinement times, and the gradual emergence of

the tokamak alternative line by the Soviets (historical irony!). Crudely speaking, the tokamak configuration cures the main problems of the  $z$ -pinch (its instability due to the curvature of the transverse magnetic field in the absence of a stabilising longitudinal magnetic field backbone) and of the  $\theta$ -pinch (its end losses), both destroying the configuration on the  $\mu s$  time scale, by combining them into a single scheme: The magnetic field is helical (with poloidal and toroidal components) and the vessel is a torus rather than a straight tube. Whereas this simply eliminates the end-loss problem of the  $\theta$ -pinch, it is not quite true that the kink instability problem of the  $z$ -pinch is eliminated as well. Instead, the basic MHD problem of tokamak confinement turns out to be a delicate balance between equilibrium considerations, favouring a large toroidal current, and stability considerations, which favour a minimum current so as to eliminate the driving force of the kink instabilities.

## 2 Cylindrical preliminaries

Some of the peculiarities of equilibrium theory may already be seen from the analysis of straight plasma cylinders with a circular cross-section. In circular cylinder symmetry,  $\partial/\partial\theta = 0$  and  $\partial/\partial z = 0$ , so that the equilibrium is a function of the radius  $r$  alone. Moreover, one easily finds from Eqs. (1)–(3) that  $B_r = 0$  and  $j_r = 0$ . As always, in static equilibria, the density profile is not determined by any condition so that  $\rho(r)$  is completely arbitrary. The remaining equilibrium functions  $p(r)$ ,  $B_\theta(r)$ ,  $B_z(r)$  are restricted to satisfy just one ODE:

$$\frac{d}{dr} \left( p + \frac{B^2}{2\mu_0} \right) = -\frac{B_\theta^2}{\mu_0 r}, \quad (4)$$

so that two of them can be chosen freely! The current density is then determined by Ampère’s law:

$$j_\theta = -\frac{1}{\mu_0} \frac{dB_z}{dr}, \quad j_z = \frac{1}{\mu_0 r} \frac{d(rB_\theta)}{dr}. \quad (5)$$

This completes the description of cylindrical equilibria. In conclusion, in addition to the density, there are two more arbitrary functions which can be freely chosen. This generates the experimental freedom to create the different configurations like  $\theta$ -pinch and a  $z$ -pinch (Fig. 1). This freedom is also present in toroidal equilibria. It will be a cause of concern there (Sec. 3).

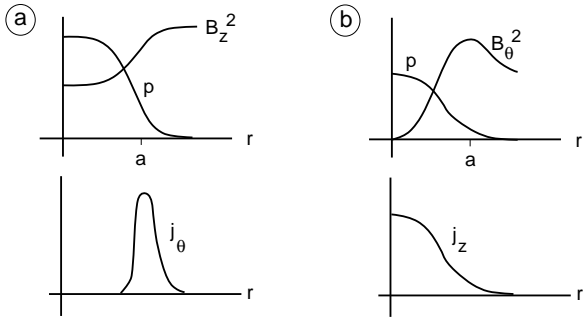


Figure 1: Typical equilibrium profiles for  $\theta$ - and  $z$ -pinch.

Except for the freedom of choice of equilibrium profiles, two more properties of toroidal configurations can be anticipated in the context of straight cylinder theory. These have to do with the global magnetic field line geometry (safety factor) and the bulk forces (magnetic pressure).

The *safety factor* is a measure for the average pitch of the magnetic field lines, i.e. the advancement in the toroidal direction after one poloidal revolution of the field lines around the plasma. We approximate a torus with *inverse aspect ratio*

$$\epsilon \equiv a/R_0 \ll 1, \quad (6)$$

where  $a$  is the minor (or the plasma) radius and  $R_0$  is the major radius of the torus, as a periodic cylinder of length  $L = 2\pi R_0$  and radius  $a$ . The nested magnetic surfaces are then represented by nested cylinders of radius  $r \leq a$ . On each of those cylinders the safety factor  $q(r)$  is easily visualised by unfolding the cylinder (Fig. 2a). Its value is given by:

$$q_{\text{cyl}} = \frac{1}{2\pi} \oint \frac{d\varphi}{d\theta} \Big|_{\text{f.l.}} d\theta = \frac{rB_z}{R_0 B_\theta} \left[ = \frac{2\pi r^2 B_z}{\mu_0 R I_\varphi} \right], \quad (7)$$

where  $\varphi \equiv 2\pi z/L$  is the toroidal angle and the expression in square brackets indicates the (confusing!) relation of  $q$  with the toroidal plasma current.

Traditionally, the name safety factor has been in use for the parameter  $q$  because stability with respect to internal kink modes in tokamaks requires  $q(\text{axis}) > 1$ , whereas stability with respect to external kink modes requires  $q(\text{boundary}) > 1$ . The latter criterion translates into a condition on the total toroidal current

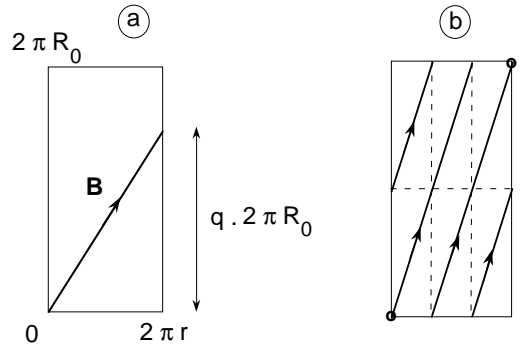


Figure 2: a. Cylindrical safety factor ( $q < 1$ ); b. Rational field line ( $q = 3/2$ ).

$I_{\text{tor}} \equiv I_\varphi(r = a)$  called the *Kruskal-Shafranov limit*, which corresponds precisely with  $q(a) = 1$ . The fact that  $q = 1$  also corresponds to a topology where the field lines close on themselves after one revolution the short way and one revolution the long way around the torus is an unfortunate coincidence which has been the source of much confusion in the literature. The point is that this topological property of the field lines has nothing to do with external kink mode stability in a genuine torus. These modes are driven by the toroidal current, as expressed by the simple relationship  $q \sim (I_{\text{tor}})^{-1}$  of Eq. (7), but the threshold for stability no longer coincides with integer values of  $q$  in general toroidal systems.

An important concept in (local) plasma stability theory is that of *rational magnetic field lines on a rational magnetic surface*. The latter is a surface (in this case a cylinder of a certain radius) where the field lines close upon themselves after  $M$  revolutions the short way and  $N$  revolutions the long way around the torus (Fig. 2b), so that the safety factor is a rational number there:

$$q_r = \frac{N}{M} \quad \left( \begin{array}{l} \text{(tor. rev.)} \\ \text{(pol. rev.)} \end{array} \right). \quad (8)$$

If  $q$  is irrational the field lines do not close on themselves and just cover the magnetic surface ergodically. The importance of rational field lines can be seen from the expression of magnetic perturbations on a rational magnetic surface. Expressing the doubly periodic perturbations in the form of an expansion in Fourier components

$$\xi \sim e^{i(m\theta + n\varphi)}, \quad (9)$$

where  $m$  is the poloidal mode number and  $n \equiv k_z R_0$  is the toroidal mode number, the main field line bending contribution is represented by the parallel gradient operator,

$$\mathbf{B} \cdot \nabla \xi \sim \mathbf{k} \cdot \mathbf{B} \xi \sim (m + nq) \xi. \quad (10)$$

Since field line bending is associated with a huge increase of the potential energy, this term must vanish, or be small, for almost all instabilities to occur. The expression vanishes when  $\mathbf{k} \cdot \mathbf{B} = 0$ , i.e. when the wave fronts of the perturbation on the magnetic surface are parallel to the magnetic field lines. According to Eq. (10) this happens when the ratio of mode numbers is rational, which is only possible on a rational surface where *the field lines are resonant with the perturbation*:

$$q_r = -\frac{m}{n} \quad \begin{array}{l} \text{(pol. mode \#)} \\ \text{(tor. mode \#)} \end{array}. \quad (11)$$

It is to be stressed that all of local MHD stability theory (giving rise to the cylindrical Suydam criterion, to the toroidal Mercier criterion, and to ballooning mode theory) centres about the existence of resonant surfaces and field lines. [Therefore, if such resonances are forbidden because of different longitudinal boundary conditions, like line-tying of solar coronal flux tubes at the photospheric boundary, stability theory is completely changed and much more stable configurations are encountered; see Goedbloed and Halberstadt, *Astronomy and Astrophysics* **286**, 265–301 (1994).]

Another, more brutal, effect that can be appreciated from a leading order cylindrical description is that of *magnetic pressure*. Since

$$\beta \equiv \frac{2\mu_0 p}{B^2} \ll 1 \quad (12)$$

for tokamaks, the total pressure is dominated by the contribution of the magnetic field:

$$P \equiv p + \frac{B^2}{2\mu_0} \approx \frac{B^2}{2\mu_0}. \quad (13)$$

One gets an impression of the magnitude of this pressure by just inserting typical values of tokamaks, e.g. for  $B = 3 \text{ T}$  one gets

$$P = 3.6 \times 10^6 \text{ N/m}^2 = 360 \text{ metric tons} = 36 \text{ atm}!$$

Clearly, magnetic forces are huge and need to be balanced very carefully. It is to be noted though that the dominant contribution of the above pressure is exerted on the external coils of the tokamak which, therefore, need a very strong supporting structure. The internal pressures, even though smaller by an order of magnitude, are not negligible either (e.g., for  $\beta = 3\%$  the plasma pressure  $p \approx 1 \text{ atm}$ ). Moreover, since  $\beta$  is a figure of merit for future fusion reactors, there is a constant drive to increase its value. This implies that part of the huge magnetic pressure estimated above will shift towards the plasma interior to resemble the  $\theta$ -pinch configuration of Fig. 1a. However, within tokamak confinement, the best one can do is reach values of  $\beta \sim \epsilon$

so that pressure effects are necessarily limited to levels which imply that the toroidal geometry plays an essential role in overall pressure balance. Obviously, this is not well described by cylindrical theory.

### 3 Grad-Shafranov equation

We have seen that two arbitrary physical profiles appear in cylindrical equilibria whereas a third profile is determined by an ODE. In axisymmetric toroidal equilibria this arbitrariness remains whereas the ODE is replaced by a PDE, the Grad-Shafranov equation. We will concentrate on the derivation of this equation and on its scaling properties. The purpose of this exercise is to derive the minimum number of dimensionless  $\mathcal{O}(1)$  quantities so that the Grad-Shafranov equation is simplified and the parameters and profiles are uniquely classified.

#### Derivation

1) The poloidal field & current are derived from *stream functions*  $\Psi(R, Z)$  &  $I(R, Z)$ :

$$\begin{aligned} \nabla \cdot \mathbf{B} &= \frac{1}{R} \frac{\partial(RB_R)}{\partial R} + \frac{\partial B_Z}{\partial Z} = 0 \\ \implies B_R &= -\frac{1}{R} \frac{\partial \Psi}{\partial Z}, \quad B_Z = \frac{1}{R} \frac{\partial \Psi}{\partial R}, \end{aligned} \quad (14)$$

$$\begin{aligned} \mathbf{j} = \nabla \times \mathbf{B} \quad \Rightarrow \quad \nabla \cdot \mathbf{j} &= \frac{1}{R} \frac{\partial(Rj_R)}{\partial R} + \frac{\partial j_Z}{\partial Z} = 0 \\ \implies j_R &= \frac{1}{R} \frac{\partial I}{\partial Z}, \quad j_Z = -\frac{1}{R} \frac{\partial I}{\partial R}. \end{aligned} \quad (15)$$

2) The poloidal & toroidal components of Ampere's law  $\mathbf{j} = \nabla \times \mathbf{B}$  provide expressions for  $I$  and  $Rj_\varphi$ :

$$\begin{aligned} j_R &= \frac{\partial B_\varphi}{\partial Z}, \quad j_Z = -\frac{1}{R} \frac{\partial(RB_\varphi)}{\partial R} \\ \implies I &\equiv RB_\varphi, \end{aligned} \quad (16)$$

$$Rj_\varphi = R \frac{\partial}{\partial R} \frac{1}{R} \frac{\partial \Psi}{\partial R} + \frac{\partial^2 \Psi}{\partial Z^2} \equiv \Delta^* \Psi. \quad (17)$$

3) The toroidal & poloidal components of the pressure balance equation  $\mathbf{j} \times \mathbf{B} = \nabla p$  imply that  $I$  and  $p$  are flux functions which are related to  $j_\varphi$ :

$$\begin{aligned} \frac{\partial p}{\partial \varphi} &= j_R B_Z - j_Z B_R = \frac{1}{R^2} \left( \frac{\partial I}{\partial Z} \frac{\partial \Psi}{\partial R} - \frac{\partial I}{\partial R} \frac{\partial \Psi}{\partial Z} \right) = 0 \\ \implies I &\equiv I(\Psi), \end{aligned} \quad (18)$$

$$\begin{aligned} \frac{\partial p}{\partial R} &= j_Z B_\varphi - j_\varphi B_Z = \left( -\frac{II'}{R^2} - \frac{j_\varphi}{R} \right) \frac{\partial \Psi}{\partial R} \\ \frac{\partial p}{\partial Z} &= j_\varphi B_R - j_R B_\varphi = \left( -\frac{II'}{R^2} - \frac{j_\varphi}{R} \right) \frac{\partial \Psi}{\partial Z} \\ \implies p &= p(\Psi), \quad -\frac{II'}{R^2} - \frac{j_\varphi}{R} = p'. \end{aligned} \quad (19), (20)$$

4) Summarising:

– From Eqs. (17) and (20) it follows that the equilibrium is described by an elliptic non-linear PDE, the *Grad-Shafranov equation*:

$$R \frac{\partial}{\partial R} \frac{1}{R} \frac{\partial \Psi}{\partial R} + \frac{\partial^2 \Psi}{\partial Z^2} = -II' - R^2 p' [= Rj_\varphi], \quad (21a)$$

which has to satisfy the boundary condition

$$\Psi = \text{const} \quad (\text{on the plasma cross-section}). \quad (21b)$$

[A hair in the soup is that this plasma cross-section, in general, is also unknown since it is determined by another non-linear problem, viz. the external free-boundary problem with given currents in external coils. Here, we will simply assume that this problem is solved separately so that the cross-sectional shape is known.]

– From Eqs. (16), (18), (19) it follows that the RHS of Eq. (21a) contains two completely arbitrary profiles:

$$I \equiv RB_\varphi = I(\Psi), \quad p = p(\Psi). \quad (22)$$

– Everything else is determined, e.g. the poloidal field and current from Eqs. (14) and (15):

$$\mathbf{B}_p = \frac{1}{R} \mathbf{e}_\varphi \times \nabla \Psi, \quad \mathbf{j}_p = -I' \mathbf{B}_p. \quad (23)$$

We will not discuss the various numerical methods of solving the boundary value problem (21) since this is a highly technical subject of interest to specialists only. It is sufficient for our purpose that accurate solutions can be generated. Instead, we will elaborate on the scaling properties since this has a general story to tell.

## Scaling

1) Construct a *minimum number of dimensionless quantities* of  $\mathcal{O}(1)$ :

Divide lengths by  $a$  and magnetic fields by  $B_0$  (the strength of the vacuum magnetic field at  $R = R_0$ ). Introduce dimensionless poloidal coordinates (Fig. 3)

$$x \equiv (R - R_0)/a, \quad y \equiv Z/a, \quad (24)$$

the inverse aspect ratio

$$\epsilon \equiv a/R_0 \quad (\ll 1 \text{ in asymptotic expansions}), \quad (25)$$

a *unit flux label* ( $\Psi_1$  is the total poloidal flux)

$$\psi \equiv \Psi/\Psi_1 \quad \Rightarrow \quad 0 \leq \psi \leq 1, \quad (26)$$

and a *dimensionless inverse flux*:

$$\alpha \equiv a^2 B_0 / \Psi_1 \quad (\text{related to } q_1 \sim \alpha). \quad (27)$$

2) With new dimensionless profiles

$$P = P(\psi) \equiv \frac{\alpha^2}{\epsilon B_0^2} p(\Psi),$$

$$Q = Q(\psi) \equiv -\frac{\epsilon \alpha^2}{a^2 B_0^2} \frac{1}{2} [I^2(\Psi) - R_0^2 B_0^2], \quad (28)$$

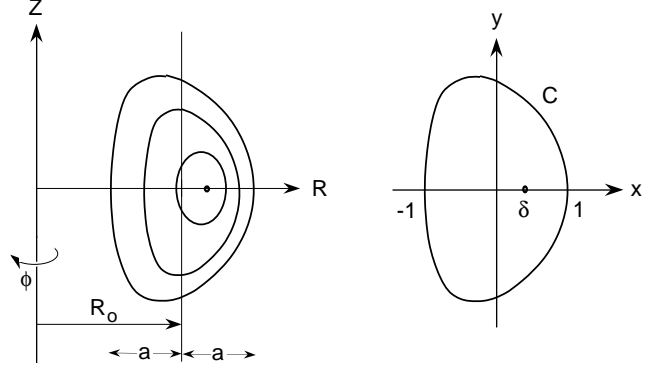


Figure 3: Cross-sectional shape and poloidal  $x$ - $y$  plane.

the Grad-Shafranov equation becomes:

$$\psi_{xx} + \psi_{yy} - \frac{\epsilon}{1 + \epsilon x} \psi_x = \frac{Q' - (1 + \epsilon x)^2 P'}{\epsilon}. \quad (29)$$

3) Introducing yet another profile to get an  $\mathcal{O}(1)$  RHS (which expresses the above-mentioned fact that tokamaks at ‘high’  $\beta \sim \epsilon$  become  $\theta$ -pinch like so that the pressure and diamagnetism should nearly balance),

$$G = G(\psi) \equiv -\frac{1}{\epsilon} [Q(\psi) - P(\psi)], \quad (30)$$

the Grad-Shafranov equation transforms to the desired form where all terms are  $\mathcal{O}(1)$  quantities:

$$\psi_{xx} + \psi_{yy} - \frac{\epsilon}{1 + \epsilon x} \psi_x = -G' - (2x + \epsilon x^2) P'. \quad (31)$$

4) We are not content yet: The profiles  $G'(\psi)$  and  $P'(\psi)$  are arbitrary, which makes it hard to compare e.g. experimental and theoretical stability results obtained with different equilibria. We should separate the amplitudes of these functions (which are related to global parameters like  $\langle \beta \rangle$  and  $q_1$ ) and the shapes. Therefore, introduce *unit profiles* and amplitudes  $A$  and  $B$ :

$$\begin{aligned} G' &\equiv -A\Gamma(\psi), & \Gamma(0) &= 1, & \Gamma(1) &= 0, \\ P' &\equiv -\frac{1}{2}AB\Pi(\psi), & \Pi(0) &= 1, & \Pi(1) &= 0. \end{aligned} \quad (32)$$

The Grad-Shafranov equation then becomes:

$$\begin{aligned} \psi_{xx} + \psi_{yy} - \frac{\epsilon}{1 + \epsilon x} \psi_x \\ = A \left[ \Gamma(\psi) + Bx \left( 1 + \frac{1}{2} \epsilon x \right) \Pi(\psi) \right], \end{aligned} \quad (33)$$

where  $\Gamma$  and  $\Pi$  roughly represent the shape of the current and the pressure gradient profile. This appears to be a final form of the Grad-Shafranov equation with no arbitrariness in the choice of functions.

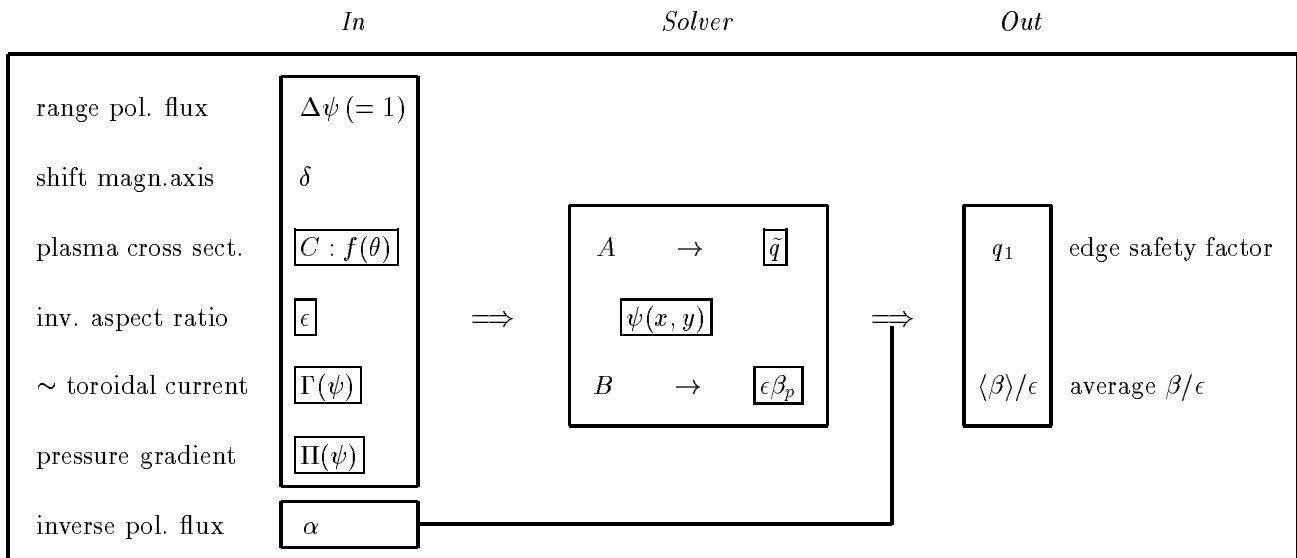


Figure 4: Independent (boxed) parameters and profiles in an equilibrium solver.

5) Finally, we formulate the boundary value problem in a non-standard way by considering the cross-sectional shape  $C$  and the position  $\delta$  of the magnetic axis (Fig. 3b) *as given* so that the boundary conditions become

$$\psi = 1 \quad \text{at plasma boundary } C \ (r = f(\theta)), \quad (34)$$

$$\psi = \psi_x = \psi_y = 0 \quad \text{at mag. axis } (x = \delta, y = 0). \quad (35)$$

However, the boundary value problem (33)–(35) is then overdetermined so that the global parameters  $A$  and  $B$  become *eigenvalues* to be determined together with the solution  $\psi$ . Effective methods exist to do this [4].

6) **Now count !!** Since the Grad-Shafranov equation is a nonlinear equation, it is not possible to distinguish between cause and effect. This translates into arbitrariness of the choice of input and output variables of the FORTRAN equilibrium code. It is essential though that the number of independent parameters and functions be carefully counted so as to enable comparison and to avoid spurious (expensive!) parameter scans. In Fig. 4 the method is summarised with respect to the choice of independent parameters and profiles of the equilibrium solver.

7) Summarising:

We have enumerated the freedom in the choice of MHD equilibrium parameters and profiles by prescribing three geometric quantities, viz. the inverse aspect ratio  $\epsilon$ , the shift  $\delta$  of the magnetic axis, and the plasma cross-sectional shape  $C$ , and two arbitrary unit profiles  $\Gamma(\psi)$  and  $\Pi(\psi)$ , corresponding to the toroidal current and the pressure gradient. Solving the Grad-Shafranov equation with these independent input parameters turns  $A$  and

$B$  into eigenvalues which are to be computed together with the solution  $\psi(x, y)$ . These parameters are directly related to the scaled physical parameters  $\tilde{q} \equiv q_1/\alpha$  and  $\epsilon\beta_p$ . The unscaled parameters  $q_1$  and  $\langle\beta\rangle/\epsilon$  (and all other parameters) are obtained by means of a trivial scaling in terms of the parameter  $\alpha$  ( $\sim \Psi^{-1}$ ), which has been scaled out of the Grad-Shafranov equation. (Hence,  $\alpha$  goes around the solver box in Fig. 4).

An important consequence of the scaling is that the product of  $\langle\beta\rangle/\epsilon$  and  $q_1^2$  is independent of  $\alpha$ , i.e. it is an intrinsic characteristic of the equilibrium. It is associated with the poloidal beta,

$$\epsilon\beta_p \sim q_1^2 \langle\beta\rangle/\epsilon, \quad (36)$$

where we have suppressed a geometric constant. This relation shows that  $\langle\beta\rangle \sim \epsilon$  and  $\beta_p \sim \epsilon^{-1}$ : the ‘high’-beta tokamak scaling. Stability studies typically involve parameter scans in the  $\langle\beta\rangle$ - $q_1$  or  $\beta_p$ - $q_1$  plane, which roughly separates equilibrium properties, described by  $\epsilon\beta_p$ , and stability properties, described by  $q_1$ .

## 4 Mapping for stability

To be able to describe perturbations with minimum field line bending it is necessary to represent the parallel gradient operator (10) very accurately. An effective way of doing this is to replace the poloidal angle  $\theta$  of Eq. (9) by a poloidal angle  $\vartheta$  such that *the field lines become straight lines* in the  $\varphi$ - $\vartheta$  plane (Fig. 5). Of course, this construction has to be carried out on each flux surface labelled by  $\psi$ . Exploiting the constructed flux variable

$\psi$  and the new angle  $\vartheta$  as coordinates for the description of instabilities requires an inversion of the coordinates:

$$\begin{aligned} \psi &= \psi(x_i, y_j) & x &= x(\psi_i, \vartheta_j), \\ \vartheta &= \vartheta(x_i, y_j) & y &= y(\psi_i, \vartheta_j). \end{aligned} \quad (37)$$

Next, all quantities occurring in the stability analysis are transformed to  $\psi, \vartheta, \varphi$  coordinates, i.e. normal field line curvature  $\kappa_n$  (involving the principal magnetic surface curvatures  $\kappa_p$  and  $\kappa_t$ ), geodesic curvature  $\kappa_g$ , toroidal current  $j_\varphi$ , etc. These involve second derivatives with respect to  $\psi$  so that the equilibrium solutions need to be surprisingly accurate for a reliable stability analysis.

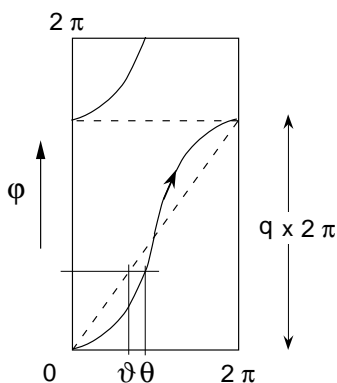


Figure 5: Construction of straight field line coordinates.

## 5 Problems and challenges

We have presented a theoretical description of toroidal equilibrium which involves the solution of the Grad-Shafranov equation and a careful choice of the parameters. The experimental counterpart is the production of *accurate* equilibrium data by means of all available diagnostics. To get agreement between these two is a long-term iterative process. The essential point is that we have not arrived yet: important parameters and profiles are only known to about 10%. Hence, tokamak diagnostics are to be improved if we ever are to arrive at a satisfactory agreement between theory and experiment.

A systematic way of improving upon this situation has been called *MHD spectroscopy* [5]. Here, the frequency spectrum of MHD waves is used to obtain equilibrium information (the inverse spectral problem). This spectrum is calculated by a spectral code which is fed by equilibria obtained by fitting experimental data to get an estimate of the free profiles. This involves considerable *uncertainty* as to how to handle deviations from nested flux surfaces: see Fig. 6, taken from Ref. [6].

We have extensively discussed the problem of the *freedom* in the choice of equilibrium profiles. More substan-

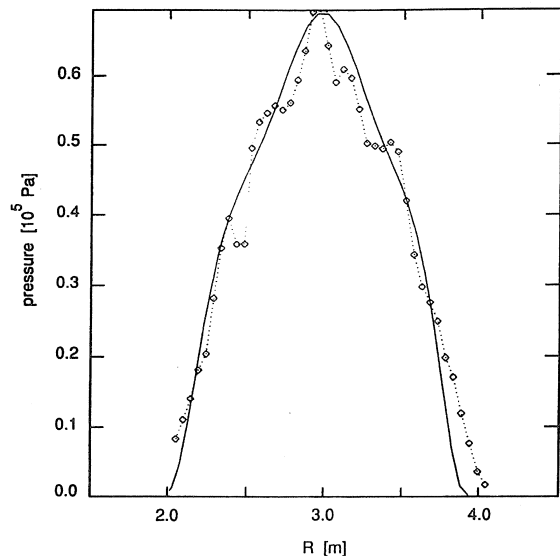


Figure 6: Uncertainty: Electron pressure profile obtained by LIDAR diagnostic at JET (dashed curve with diamonds) and reconstructed pressure profile by means of an equilibrium solver (drawn curve).

tial are problems of *three-dimensionality* of the equilibrium, associated with deviations from axisymmetry due to field errors, saturated non-linear instabilities, possibly leading to non-axisymmetric equilibrium states, stochastic field lines, etc.

Another area of study is the effect of *stationary flow* on equilibria, i.e. departure from static equilibrium due to neutral beams, pumped divertors, etc. Here, three more free equilibrium profiles appear. The problem of infinite freedom remains with us!

## References

- [1] J.P. Freidberg, *Ideal Magnetohydrodynamics* (Plenum Press, New York, 1987).
- [2] J. Wesson, *Tokamaks*, 2nd edition (Clarendon Press, Oxford, 1996).
- [3] J.P. Goedbloed and S. Poedts, *Principles of Magnetohydrodynamics* (Cambridge University Press, Cambridge, 2004).
- [4] J.P. Goedbloed, *Comp. Phys. Comm.* **31**, 123–135 (1984); *Err.:* *Comp. Phys. Comm.* **41**, 196 (1986).
- [5] J.P. Goedbloed, G.T.A. Huysmans, H. Holties, W. Kerner, S. Poedts, *Plasma Physics and Controlled Fusion* **35**, B277–292 (1993).
- [6] G.T.A. Huysmans, J.P. Goedbloed, W. Kerner, *Physics of Fluids* **B5**, 1545–1558 (1993).